

## The tolerability of dextran-coated iron oxide nanoparticles during *in vivo* observation of the rats

Cristina L. Popa<sup>1</sup>, Alina M. Prodan<sup>2,3</sup>, Carmen S. Ciobanu<sup>1</sup> and Daniela Predoi<sup>1</sup>

<sup>1</sup> National Institute of Materials Physics, P.O. Box MG 07, 07725, Magurele, Romania

<sup>2</sup> Emergency Hospital Floreasca, Calea Floresca 8, Bucharest, Romania

<sup>3</sup> Carol Davila University of Medicine and Pharmacy, 8 Eroii Sanitari, Bucharest, Romania

**Abstract.** Superparamagnetic iron oxide nanoparticles (SPION) have attracted a lot of interest due to their widespread biomedical and diagnostic applications. Coating the SPIONs with various surface layers can provide an interface between the core and the surrounding environment. The aim of this study was to examine the *in vivo* behaviour of dextran-coated iron oxide nanoparticles (D-IONPs) in aqueous suspensions. The SPIONs stabilized with dextran (D-IONPs) were synthesized in aqueous solutions by co-precipitation method. The average grain size deduced from transmission electron microscopy is 7.5 nm. The hematological parameters registered for the rats exposed to D-IONPs at 1 ml/kg have had values approximately equal to those examined for the control specimen. The architecture of liver and kidneys was not affected after one day of intraperitoneal injection of D-IONPs compared to the reference group. After 21 and 28 days respectively from the administration of the D-IONPs solution, the liver and kidneys from the injected rats showed a normal aspect without abnormalities compared to the rats uninjected. Our findings suggest that the administration of 1 ml/kg D-IONPs did not cause any toxicological effect since the parameters of renal and liver function were in the normal range as reported to the control group.

**Key words:** Blood biochemical assay — Hematological parameters — Tolerability

**Abbreviations:** ALT, alanine aminotransferase; AST, aspartate aminotransferase; BUN, blood urea nitrogen; CRE, creatinine; D-IONPs, dextran-coated iron oxide nanoparticles; DLS, dynamic light scattering; Hct, hematocrit; Hgb, hemoglobin; RBC, red blood cells; SAED, selected area electron diffraction; SPION, superparamagnetic iron oxide nanoparticles; TEM, transmission electron microscopy; WBC, white blood cells.

### Introduction

In the last years, the superparamagnetic iron oxide nanoparticles (SPION) have attracted a lot of interest due to their widespread biomedical and diagnostic applications (Berry et al. 2003; Pankhurst et al. 2003; Tartaj et al. 2003; Bautista et al. 2005). Due to the special magnetic properties as well as their biocompatibility and non-toxicity, SPIONs can be used in molecular imaging. On the other hand, the specific properties of these nanoparticles enable them to

bind to a range of drugs, proteins, peptides, antibodies, polymers, DNA, RNA, oligosaccharides, etc. (Kinsella and Ivanisevic 2005; Lee et al. 2006; Yigit et al. 2008; Laurent and Mahmoudi 2011; Chen et al. 2012). Due to the fact that the surface/volume ratio increases when the size decreases, these particles facilitate conjugation with various molecular markers, which can interact at molecular and cellular levels. Generally, this kind of nanoparticles are formed of a magnetic core which consists of maghemite ( $\gamma$ -Fe<sub>2</sub>O<sub>3</sub>) or magnetite (Fe<sub>3</sub>O<sub>4</sub>), encapsulated in a biocompatible polymer such as dextran or sucrose (Bautista et al. 2005; Predoi and Valsangiacom 2007). Coating the SPIONs with polymer prevents their aggregation and the functional groups (e.g. -NH<sub>2</sub>, -OH) of the polymer allow

Correspondence to: Daniela Predoi, National Institute of Materials Physics, P.O. Box MG 07, 07725, Magurele, Romania  
E-mail: dpredoi@gmail.com

the conjugation with bioactive compounds such as antibodies or drugs on the SPIONs surface. The core particle size of SPIONs and the hydrodynamic particle size in the dispersion medium including the SPIONs core and polymer coating have a critical significance for *in vivo* applications (Weissleder et al. 1988; 1990; Shapiro et al. 2005; Petri-Fink and Hofmann 2007; Thorek and Tsourkas 2008). There are many synthesis methods for obtaining SPIONs with different sizes. Among them are included chemical precipitation (Predoi and Valsangiacom 2007; Huang et al. 2012; Barick et al. 2014), high temperature methods (Sun and Zeng 2002), etc. Magnetic properties of SPIONs are strongly influenced by the surface to volume ratio. In order to be used as MRI probes, the SPIONs must exhibit a high magnetization when an external magnetic field is applied and must have a well-developed surface coating and functionality (Jun et al. 2008). Coating the SPIONs with various surface layers can provide an interface between the core and the surrounding environment (Rochelle Arvizo and Rotello). In 2004, for the first time, Molday and Mackenzie synthesized the iron oxide nanoparticles coated with dextran (Paul et al. 2004).

Although it is known that for living organisms, iron is essential because it is required for many metabolic processes including oxygen transport, drug metabolism, DNA synthesis, ATP production etc. (Crichton 2004), the concentration of iron within cells must be very well controlled due to the cytotoxicity of excess iron. Moreover, in the treatment of iron-deficiency anemia, iron-saccharide complexes such as iron-dextran, iron-sucrose, iron-polysaccharide etc. are being used (Hudson and Comstock 2001; Kane et al. 2003).

The aim of this study was to examine the *in vivo* behaviour of dextran-coated iron oxide nanoparticles (D-IONPs) in aqueous suspensions after the intraperitoneal injection. The intraperitoneal injection was chosen as method of administration since it is the most commonly used way for drug administration, whereas the peritoneum offers a large surface area of the abdominal cavity. Moreover, the toxicological potential of D-IONPs was evaluated after intraperitoneal injection over a period of one month. Blood haematology parameters such as red blood cells (RBC), white blood cells (WBC), platelets, hematocrit (Hct) and hemoglobin (Hgb) were determined every week. At the same time, biochemical analysis of blood such as aspartate aminotransferase (AST), alanine aminotransferase (ALT), creatinine (CRE) and blood urea nitrogen (BUN) were also performed. Furthermore, histological investigations were achieved every 7 days.

In this paper we also report the transmission electron microscopy (TEM) and dynamic light scattering (DLS) studies on the obtained samples. For D-IONPs, the mean sizes, deduced from the TEM images have values of approximately  $7.5 \pm 0.5$  nm while the mean hydrodynamic size of D-IONPs deduced from DLS analysis was  $30 \text{ nm} \pm 0.5$  nm.

## Material and Methods

### Materials

Ferrous chloride tetrahydrate ( $\text{FeCl}_2 \times 4\text{H}_2\text{O}$ ), ferric chloride hexahydrate ( $\text{FeCl}_3 \times 6\text{H}_2\text{O}$ ), sodium hydroxide (NaOH), dextran ( $\text{H}(\text{C}_6\text{H}_{10}\text{O}_5)_x\text{OH}$ ; m.w.  $\sim 40,000$ ), hydrochloric acid (HCl), and perchloric acid ( $\text{HClO}_4$ ) were purchased from Merck. Deionized water was used in the synthesis of nanoparticles, and for rinsing the clusters.

### Synthesis of D-IONPs

Ferrous chloride tetrahydrate ( $\text{FeCl}_2 \times 4\text{H}_2\text{O}$ ) in 2 M HCl and ferric chloride hexahydrate ( $\text{FeCl}_3 \times 6\text{H}_2\text{O}$ ) ( $\text{Fe}^{2+}/\text{Fe}^{3+} = 1/2$ ) were mixed at  $40^\circ\text{C}$ . The mixture was dropped into dextran (30 g in 100 ml of water) and 300 ml of NaOH (2 mol/l) solution at room temperature under vigorous stirring for about 30 min. The resulting solution was heated at  $90^\circ\text{C}$  for 1 h under continuous stirring (200 rot/min). The 5 M NaOH solution was added drop by drop to obtain a pH 11. The precipitate was centrifuged and treated repeatedly with a perchloric acid (3 mol/l) solution until the  $\text{Fe}^{2+}/\text{Fe}^{3+}$  ratio in the bulk sample was approximately 0.05 (Predoi 2007).

After the last separation by centrifugation, the aqueous suspension of iron nanoparticles was dispersed into dextran (30 g in 100 ml of water). The final D-IONPs was heated at  $90^\circ\text{C}$  for 1 h under continuous stirring (200 rot/min). The solution containing D-IONPs was washed by means of magnetic columns. Finally, the D-IONPs suspension was obtained. The final iron concentration in D-IONPs solution was 0.38 mol/l. To determine the amount of iron, potassium dichromate ( $\text{K}_2\text{Cr}_2\text{O}_7$ ) was used. The  $\text{Fe}^{2+}$  was titrated potentiometrically with  $\text{K}_2\text{Cr}_2\text{O}_7$  (Iconaru et al. 2012). After the reduction of iron by  $\text{SnCl}_2$  (stannous chloride), the total Fe content was determined.

### Methods

The particle size was measured by the SZ-100 Nanoparticle Analyzer (Horiba) using DLS. The signal obtained from the scattered light is fed into a multi-channel correlator that generates a function used to determine the translational diffusion coefficient of the analyzed particles. The Stokes-Einstein equation was then used to calculate the particle size. TEM studies were carried out using a JEOL 200 CX. The specimen for TEM imaging was prepared from the particle suspension in deionized water. A drop of well-dispersed supernatant was placed on a carbon-coated 200 mesh copper grid, followed by drying the sample at ambient conditions before attaching it to the sample holder on the microscope. A superconducting quantum interference device (SQUID),

Quantum Design MPMS) magnetometer was used to record the magnetization curves of D-IONPs.

### Animals

Male Brown Norway rats (weighing 200 g) were provided by the National Institute of Research and Development for Microbiology and Immunology “Cantacuzino”, Bucharest. Female rats were not used in this study due to hormonal (estrogen/progesterone) fluctuations during their menstruation cycle. The fluctuations of these hormones may influence the blood analysis results and the actual results of the experiment (Rando and Wahli 2011). The rats were housed in stainless steel cages (four rats in every cage), with free access to food and water *ad libitum*. The rats were acclimated in controlled environmental conditions, with preset temperature ( $22 \pm 2^\circ\text{C}$ ), light (12 h light/dark cycles) and humidity ( $60 \pm 10\%$ ). Before the beginning of the experiment, the rats were kept in the laboratory one week for acclimatization. The animals were maintained under specific pathogen-free conditions in accordance with the International Animal Care Policies and with NIH Guide for the Care and Use of laboratory Animals.

### Hematology analysis and blood biochemical assay

For hematology analysis and blood biochemical assay, blood samples were collected from the rat's tail vein. The blood was collected in EDTA microtainer tubes and stored in a refrigerator at 2 to  $8^\circ\text{C}$ . The samples were analyzed in the first 2 hours of collection. In this study, hematologic parameters such as RBC, WBC, platelets, Hct and Hgb were investigated. On the other hand, liver function was evaluated by AST and ALT. Moreover, by CRE and BUN, the nephrotoxicity was determined. All the parameters were evaluated every week using a IDEXX VetAutoread Hematology Analyzer.

### Histological examination

The analysis of D-IONPs tolerability during *in vivo* long-term experiments was evaluated after the rats ( $n = 10$  rats *per* group) were injected with D-IONPs in doses of 1 ml/kg *per* rat. One group served as control group. After intraperitoneal injection of D-IONPs, the toxicity was evaluated during the entire study period. For histopathological examinations, the animals were euthanized. Histopathological examinations were performed on liver, kidney and spleen tissues.

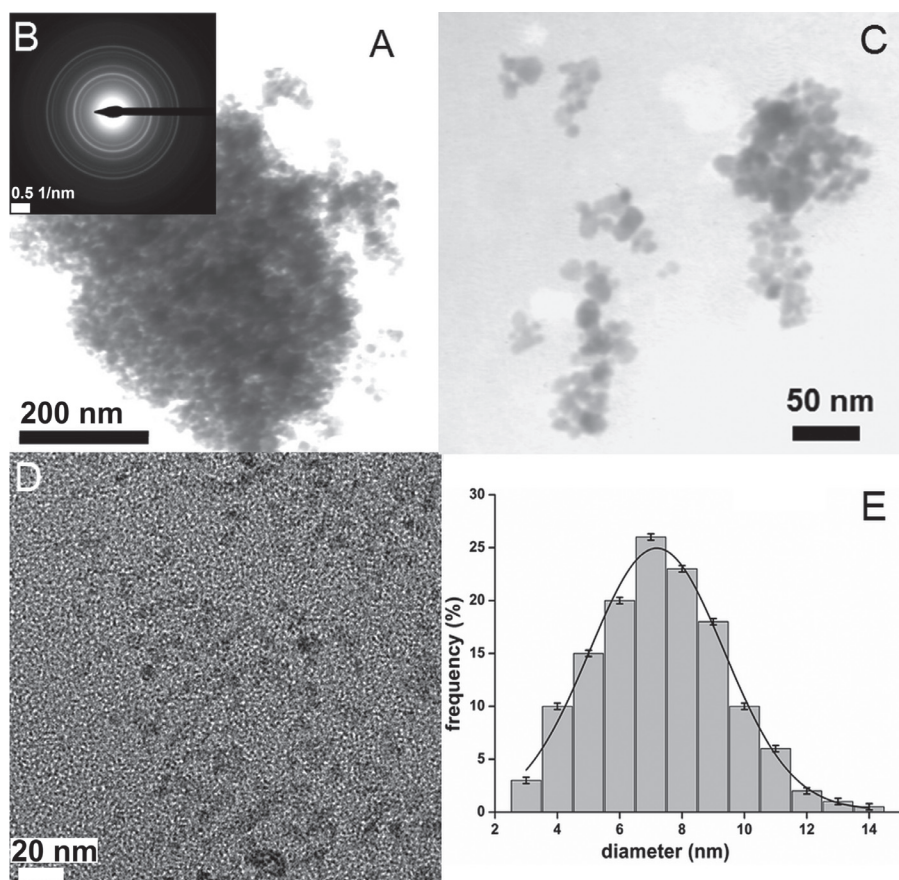


**Figure 1.** The shape of the nanoparticles, selected area electron diffraction (SAED) and size distribution of D-IONPs measured from low-magnification TEM micrograph. **A.** Large-area TEM (200 nm) image of D-IONPs. **B.** SAED pattern from a region comprised of a large number of nanoparticles. **C.** Higher magnification TEM (50 nm) image of D-IONPs. **D.** Higher magnification TEM (20 nm) image of D-IONPs. **E.** Size distribution of D-IONPs.

The selected organs were removed from the rats and fixed in 10% formalin. The organs were prepared as paraffin-embedded glass slides stained with hematoxylin and eosin. The morphological changes were observed by microscope (Daffodil MCX100 Microscope by Micros, Austria) (Su et al. 2012). The body weight was determined every week and the histopathological examinations were carried out every 7 days for a period of one month.

## Results

The shape of the nanoparticles, selected area electron diffraction (SAED) and size distribution of D-IONPs measured from low-magnification TEM micrograph are shown in Figure 1. Fig. 1A revealed a low-magnification TEM image of D-IONPs. The inset (Fig. 1B) is a SAED pattern from a zone comprised of a large number of nanoparticles. The rings in the SAED pattern can be indexed as the 220, 311, 400, 422, 511 and 440 reflections of the cubic maghemite. Fig. 1C and Fig. 1D show the higher magnification TEM images of D-IONPs. The D-IONPs observed in the higher magnification TEM image clearly suggest that the nanoparticles are uniform with a spherical shape. The size distribution was determined by measuring the mean diameter,  $D$ , of approximately 700 particles. The average grain size of the monodisperse D-IONPs was  $7.5 \pm 0.5$  nm.

Dynamic light scattering known as Quasi-Elastic Light Scattering was used to determine the hydrodynamic size and the size distribution profile of D-IONPs in suspension (Fig. 2). The intensity distribution of particle sizes obtained by DLS showed two populations. The second population was

represented by the aggregate population containing a few dozen particles but is not significant for the total quantity. Therefore, we can say that the aggregation state of the particles was minimal. The first population presented a size characteristic to a solvated particle. The size obtained by DLS was given by the crystalline area and by the thickness of the solvation layer. The average diameter obtained by DLS was  $10.3 \pm 4.5$  nm.

D-IONPs observed by DLS are monodisperse in water (Fig. 2). The mean hydrodynamic size of D-IONPs deduced from the size distribution histogram was  $30 \text{ nm} \pm 0.5 \text{ nm}$ .

The magnetization curves of D-IONPs recorded at room temperature are shown in Fig. 3. The D-IONPs exhibited superparamagnetic behaviour. The saturation magnetization ( $M_S$ ) of D-IONPs was  $27 \text{ emu/g}$ . According to previous studies (Elliott et al. 1984; Zhang et al. 2011), the increase of the particle size leads to a decrease of the saturation magnetization. On the other hand, recent studies (Zhang et al. 2011) showed that the thickness of the layer (in our case dextran) covering the nanoparticles play an important role on the magnetic properties. According to previous studies (Zhang et al. 2011), in this case, we could say that the dextran thickness is small enough not to lead to a decrease of the magnetic strength, this being a consequence of the weight contribution from the nonmagnetic portion. The results of the magnetic properties of D-IONPs demonstrate that the compound has superparamagnetic properties and it could be used in medical applications.

In order to evaluate the tolerability of D-IONPs in a solution with the final ion concentration  $0.38 \text{ mol/l}$ , the rats were injected intraperitoneally with a  $1 \text{ ml/kg}$  dose. Firstly, the blood hematology parameters and blood biochemical

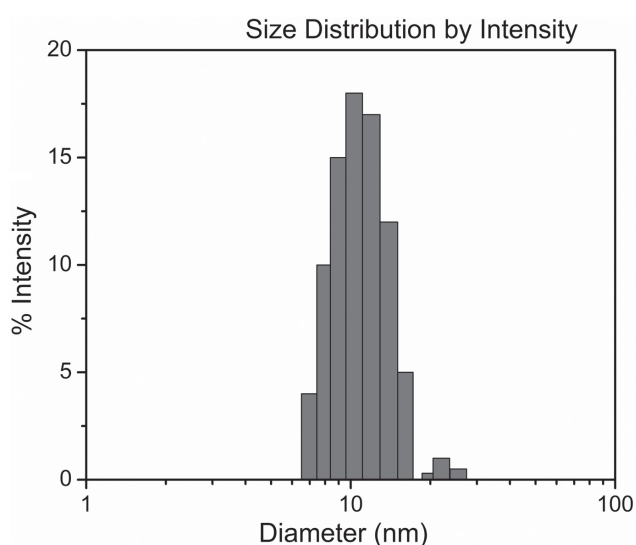


**Figure 2.** Size distribution of D-IONPs determined by dynamic light scattering (DLS).

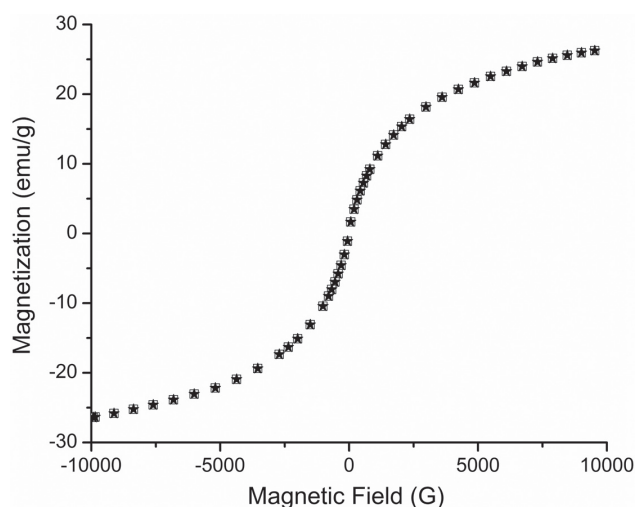


**Figure 3.** Magnetization curves of D-IONPs at room temperature.

assay of the injected rats were determined every week and compared with the control (the group of rats which was not injected). Secondly, the histological investigations on kidney and liver tissues were performed every 14 days. All the animals from all study groups survived until the end of the study period. After the intraperitoneal injection with a 1 ml/kg dose of D-IONPs containing solution, neither the weight nor the behavior of the animals was affected and no clinical signs were observed during the entire time of the experiment. All the rats from all experimental groups (treated with 1 ml/kg dose of D-IONPs containing solution) were active and nonaggressive during the interactions with other mice from the cage. The hematological analysis data for the rats injected intraperitoneally

with 1 ml/kg dose of D-IONPs containing solution are presented in Fig. 4.

On the first day after injection, an increase of the hematologic parameters such as RBC, WBC, platelet, Hct and Hgb could be observed. After 7 days, the values of RBC, WBC, platelet, Hct and Hgb decreased, being in the normal laboratory range of  $7.57\text{--}9.05 \cdot 10^{12}/\text{l}$ ,  $1.76\text{--}5.62 \cdot 10^9/\text{l}$ ,  $707\text{--}1028 \cdot 10^9/\text{l}$ ,  $40.9\text{--}46.1 \text{ l/l}$  and  $13.6\text{--}11.6 \text{ g/dl}$ , respectively. Moreover, the results obtained after the 28 days are comparable to those obtained for the rats in the control group.

In Fig. 5 are shown the values obtained for liver function evaluated by AST and ALT. The results achieved from studies of nephrotoxicity evaluated by CRE and BUN are presented in Fig. 6.

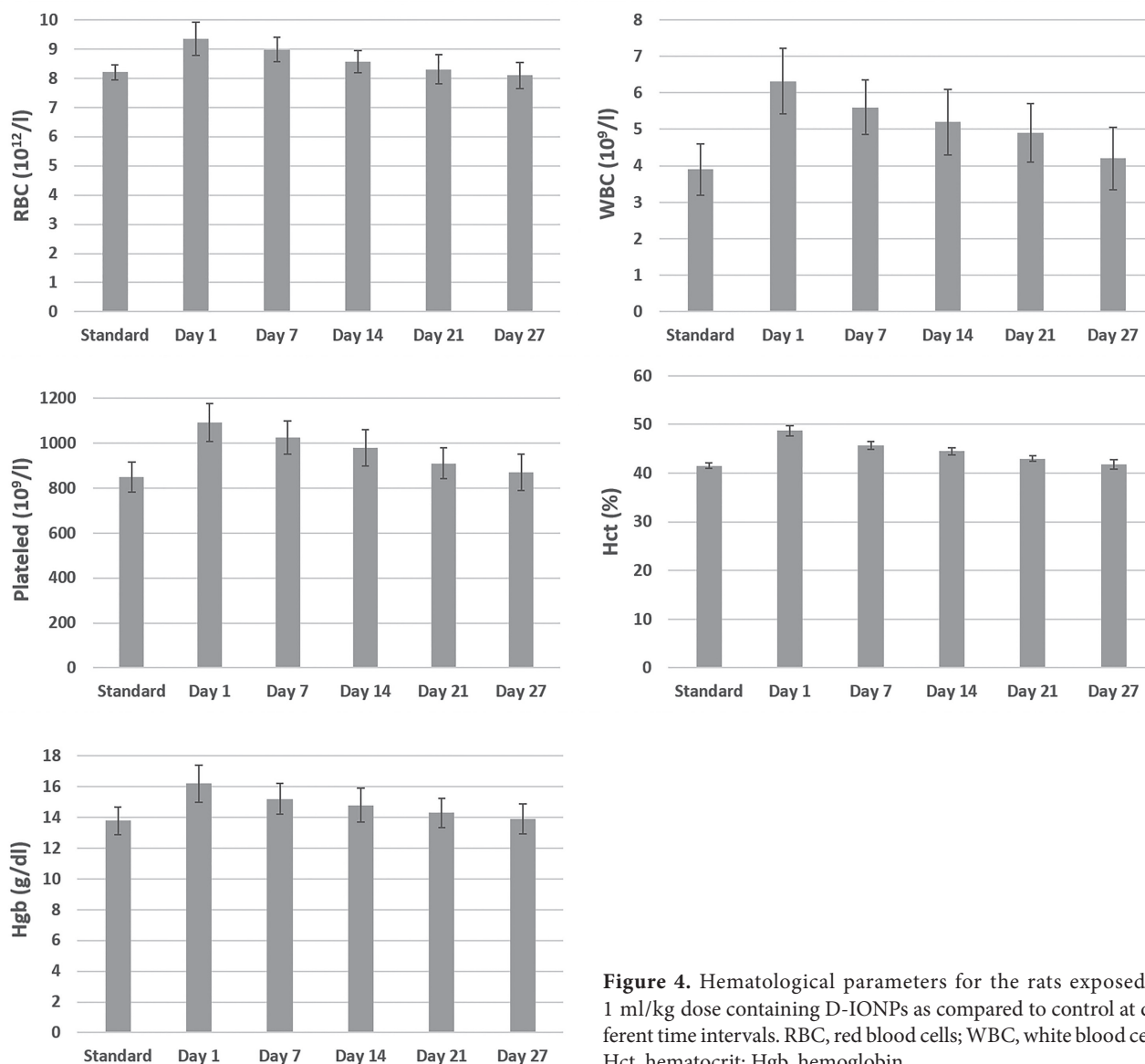


**Figure 4.** Hematological parameters for the rats exposed to 1 ml/kg dose containing D-IONPs as compared to control at different time intervals. RBC, red blood cells; WBC, white blood cells; Hct, hematocrit; Hgb, hemoglobin.

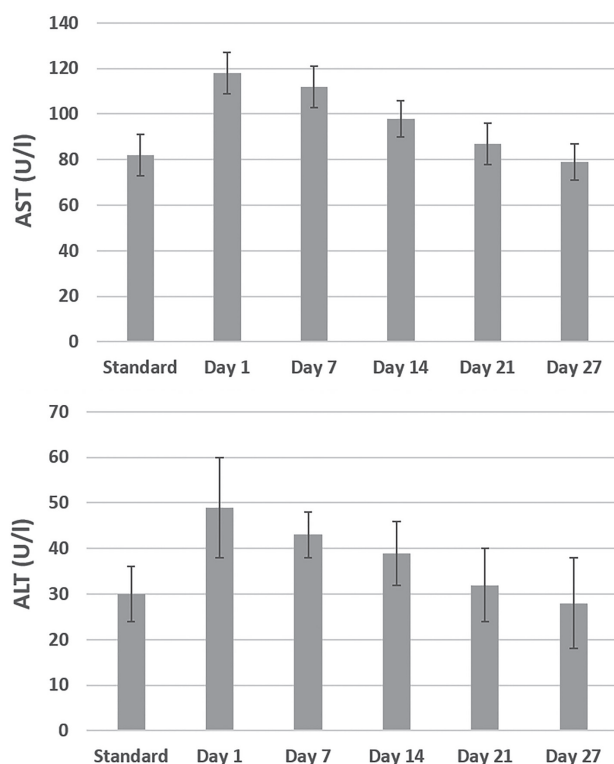


**Figure 5.** The values obtained for liver function of the rats, evaluated by aspartate aminotransferase (AST) and alanine aminotransferase (ALT).

The values of liver function evaluated by AST and ALT showed a slight increase. On the other hand, after a day, we also noticed a slight increase in the values of CRE and BUN with no significant differences relative to the normal laboratory range (AST (U/l): 45–82; ALT (U/l): 24–30; CRE ( $\mu\text{mol/l}$ ): 20–26.7; BUN (mmol/l): 3.7–6.8).

The tolerability of D-IONs in solution after intraperitoneal injection of a dose of 1 ml/kg in the studied rats was also evaluated by histological examination. Previous studies conducted by Choi et al. (2007) and Yang et al. (2007) on applications of magnetic nanoparticles in biomedicine showed that nanoparticles might have toxic effects on various organs depending on the administration method. Therefore, in this study, kidney, liver and spleen were selected as representative organs. On the other hand, Kim et al. (2006) in previous studies showed that the silica-coated magnetic nanoparticles were accumulated to various organs including liver, spleen, and kidney after intraperitoneal administration of the rats.

The microscopic observations of the rat kidney and liver tissues after intraperitoneal injection are presented in Figures 7–11. The architecture of the liver and kidney tissues was not affected one day after the intraperitoneal injection of D-IONPs compared to the reference group (Fig. 7).

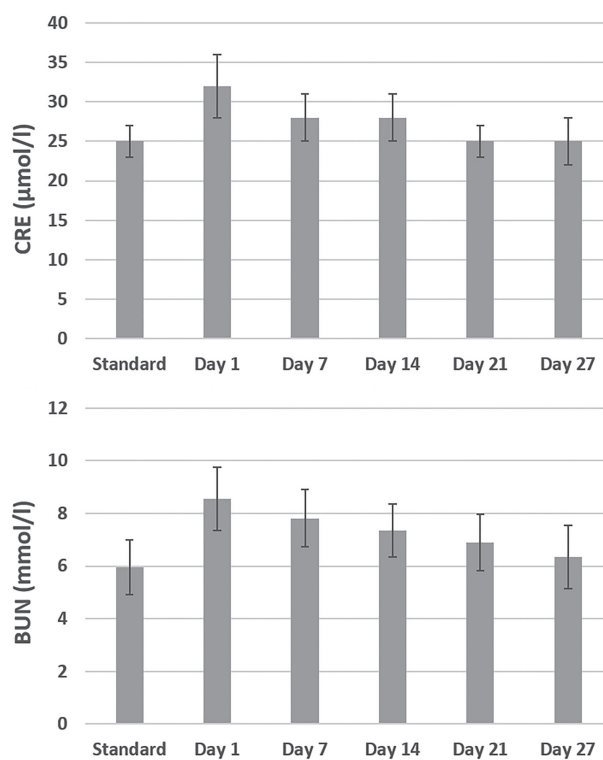


**Figure 6.** The results from nephrotoxicity studies of the rats evaluated by creatinine (CRE) and blood urea nitrogen (BUN).

The photomicrographs of kidney one day after intraperitoneal injection of D-IONPs revealed that tubular cells with moderate anisokaryosis were present. The anisochromia with formation of chromocenters and minimal granular cytoplasmic degeneration (HE, 100 $\times$ ) was also observed (Fig. 7). After one day, the histopathological examination of liver tissue of the intraperitoneally injected rats showed formation of chromocenters and nucleoli without a significant difference with the control animals group (Fig. 7).

Histopathological analysis of liver and kidney were also performed 7 days after injection (Fig. 8).

The histopathological examination of the liver showed no differences between the reference group and the groups injected intraperitoneally with D-IONPs 14 days before pre-levation (Fig. 9). In a similar way, the kidney tissue showed no abnormalities fourteen days after intraperitoneal injection of the rats with D-IONPs (Fig. 9).

The histopathological images of liver and kidney tissues harvested from the rats with or without D-IONPs injected intraperitoneally 21 (Fig. 10) and 28 (Fig. 11) days before the pre-levation, are identical.

In addition, the histopathological examination of spleen at 7, 21 and 28 days after intraperitoneal injection of D-IONPs is presented in Fig. 12. The spleen architecture consists of

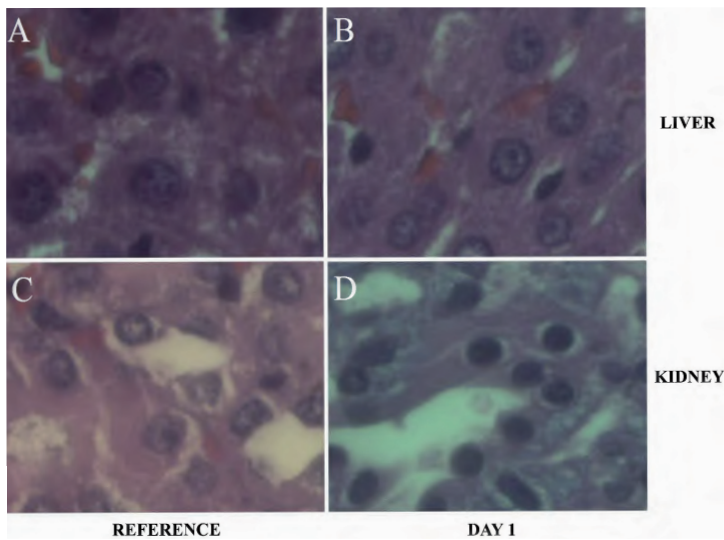


**Figure 7.** Histopathological examination of liver and kidney: liver (A) and kidney (C) control; liver (B) and kidney (D) one day after i.p. injection of D-IONPs. For staining of the sections of selected tissues hematoxylin and eosin were used. A representative tissue section of each organ was shown ( $\times 100$  magnification).

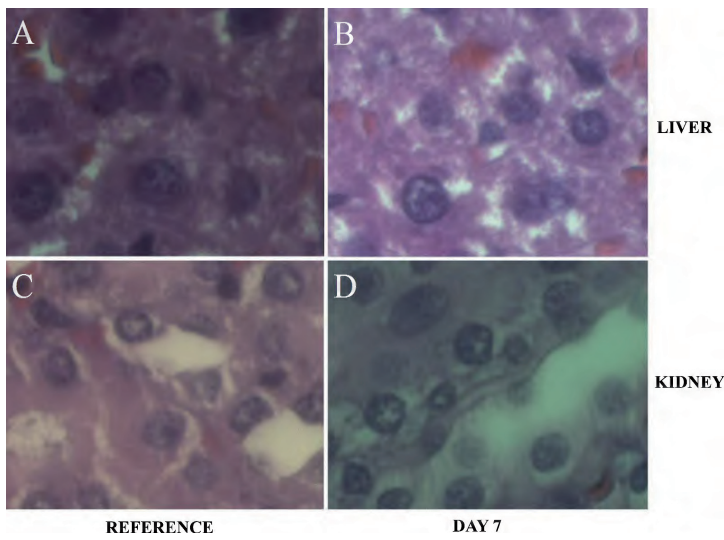


**Figure 8.** Histopathological examination of liver and kidney: liver (A) and kidney (C) control; liver (B) and kidney (D) at 7 days after i.p. injection of D-IONPs. For staining the sections of selected tissues, Hematoxylin and eosin were used. A representative tissue section of each organ was shown ( $\times 100$  magnification).

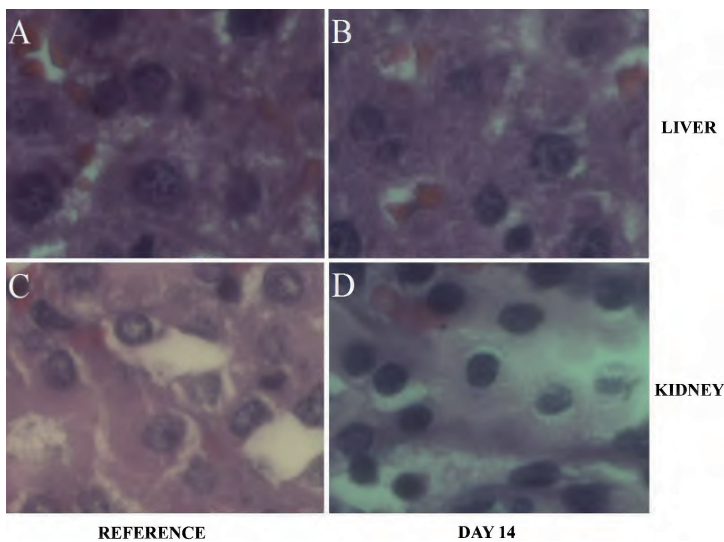


**Figure 9.** Histopathological examination of liver and kidney: liver (A) and kidney (C) control; liver (B) and kidney (D) at 14 days after i.p. injection of D-IONPs. For staining the sections of selected tissues, hematoxylin and eosin were used. A representative tissue section of each organ was shown ( $\times 100$  magnification).

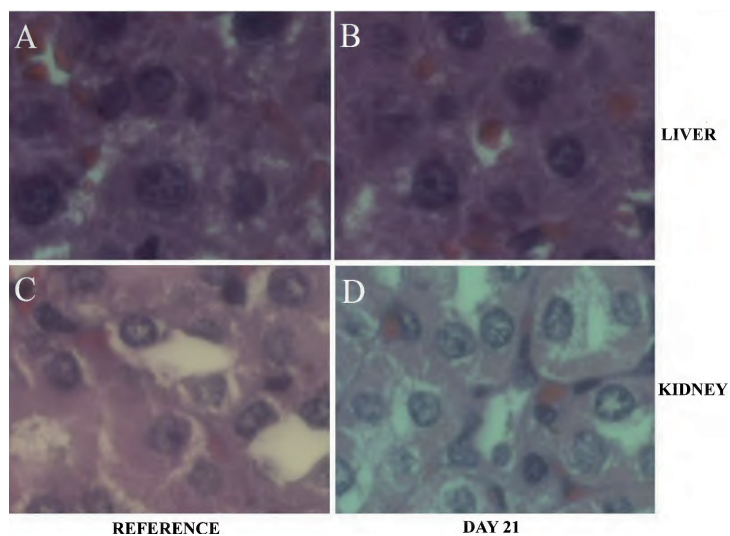


**Figure 10.** Histopathological examination of liver and kidney: liver (A) and kidney (C) control; liver (B) and kidney (D) at 21 days after i.p. injection of D-IONPs. For staining of the sections of selected tissues hematoxylin and eosin were used. A representative tissue section of each organ was shown ( $\times 100$  magnification).

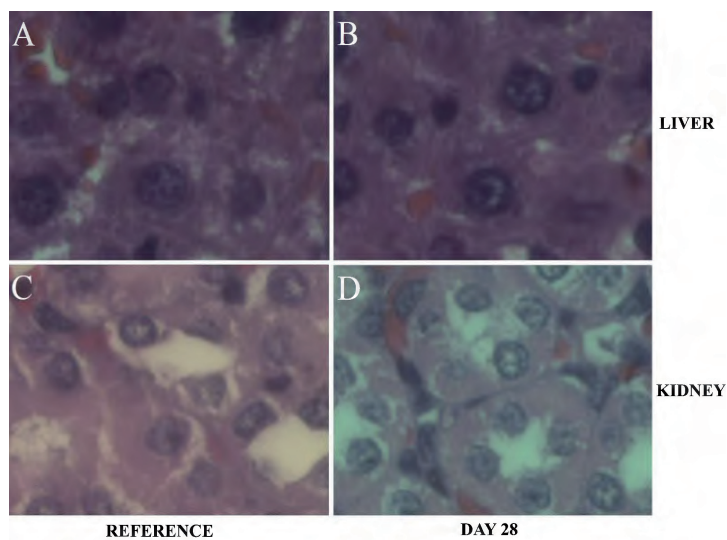


**Figure 11.** Histopathological examination of liver and kidney: liver (A) and kidney (C) control; liver (B) and kidney (D) at 28 days after i.p. injection of D-IONPs. For staining of the sections of selected tissues hematoxylin and eosin were used. A representative tissue section of each organ was shown ( $\times 100$  magnification).

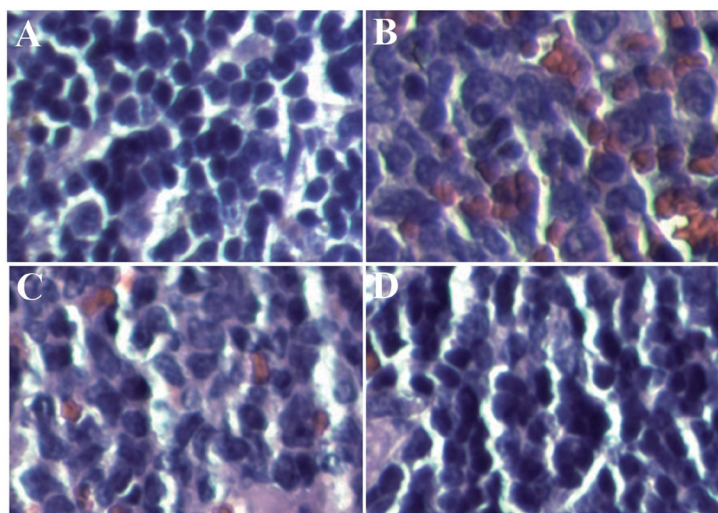


**Figure 12.** Histopathological examination of spleen tissue harvested from rats before administration D-IONPs (A) and 7 days (B), 21 days (C) and 28 days (D) after i.p. injection of D-IONPs. For staining of the sections of selected tissues hematoxylin and eosin were used. A representative tissue section of each organ was shown ( $\times 100$  magnification).

white pulp and red pulp. Small and medium sized lymphocytes were observed in the tissue harvested at different periods of time. Seven days after the injection of the D-IONPs, a massive congestion in the red pulp was observed (Fig. 12B). A significant reduction of the congestion from the red pulp was observed in the splenic tissue harvested 21 days after the injection (Fig. 12C). 28 days after the administration of D-IONPs (Fig. 12D), the spleen architecture did not present any major alterations when compared with the control (Fig. 12A).

## Discussion

In the last decade, the progress registered in the field of nanotechnology offers new opportunities for developing innovative methods for medical applications. The potential use in the medical field of superparamagnetic iron oxide particles coated with various biomolecules is of great interest, drawing the attention of many researchers. Moreover, the potential toxicology profile is intensively studied, this subject creating the premises of further research on blood purification and drug treatments for cancer and hyperthermia (Stamopoulos et al. 2007, 2008; Chen et al. 2008; Yallapu et al. 2011).

Recent studies (Huang et al. 2012; Barick et al. 2014) showed that magnetic nanoparticles have significant potential in various biological applications such as controlled drug delivery, magnetic resonance imaging or magnetic hyperthermia for cancer treatment. Yang et al. (2007) in previous studies on persistent tissue kinetics and redistribution of nanoparticles, quantum dot 705, in mice showed that after the intravenous injection of mice, quantum dots were accumulated to liver, spleen and kidneys. Moreover, Cho et al. (2009) proved that after the mice were injected intravenously, gold nanoparticles were stored in spleen and liver. Compared to intraperitoneal administration or intravenous injection, the nanoparticles present entirely distinct behavior after inhalation or instillation (Cho et al. 2007; Hara et al. 2008; Kwon et al. 2008). Cho et al. (2007) showed that the inflammatory mediators were induced by intratracheal instillation of ultrafine amorphous silica particles. On the other hand, Hara et al. (2008) in their studies exhibited that the polylactideglycolide (PLGA) nanospheres rapidly penetrate the systemic circulation and are distributed to brain, liver, kidney, pancreas and spleen after being instilled to the lungs of the rats. Furthermore, Kwon et al. (2008) in the studies on body distribution of inhaled fluorescent magnetic nanoparticles in the mice showed that after one month from administration by inhalation, the fluorescent magnetic nanoparticles were distributed in various organs such as testis, spleen, liver and even in brain.

DLS measurements gave a significantly larger size for D-IONPs in contrast to TEM measurements. According to

previous studies (Jain et al. 2005; Easo and Mohanan 2013) this is caused because the DLS method measures the hydrodynamic particle size in dispersions where the D-IONPs core and polymer coating are included, while TEM images exhibit the core particle size alone, without any contribution of the dextran layer.

Regarding the values of the parameters which represent the liver function after 1 day and 7 days respectively, the increase noticed after 24 hours cannot be considered to have some toxicological relevance.

In addition, the kidney function of rats injected intraperitoneally with a 1 ml/kg dose containing D-IONPs was not affected by the D-IONPs. Furthermore, in our present study, the blood hematology analysis results showed no abnormalities.

No significant macroscopic histopathological changes were observed between the reference group and the groups injected intraperitoneally with D-IONPs 7 days before (Fig. 8). It is notable that after 7 days no morphological alterations are presented in the liver and kidney tissues.

Compared to the histopathological images from the untreated animal group (reference), the histopathological images from the organs of injected groups, after 21 (Fig. 10) and 28 days (Fig. 11) respectively, presented similar structures with cellular and nuclear morphology. The histopathological images showed a homogeneous behavior compared to the control in all of the liver and kidney samples harvested at 21 days and 28 days respectively after intraperitoneal injection. Moreover, the liver and kidney tissues after 21 and 28 days from the intraperitoneal injection have a normal aspect without abnormalities.

According to the previous studies conducted by Handy and Shaw (2007) on the toxic effects of nanoparticles and nanomaterials, the iron nanoparticles can be toxic to the body because they can accumulate in the liver, leading to a decrease in mitochondrial activity and morphological changes. On the other hand, Handy and Shaw argued that the iron nanoparticles increase oxidative and shock reactions in liver cells and contribute to the reduction of glutathione liver cells. The results of this study showed that the effect of nanoparticles on the liver 28 days after intraperitoneal injection of D-IONPs was not visible. After 28 days, the values of liver enzymes such as ALT and AST obtained for the experimental groups are comparable to those obtained for rats in the control group. As stated by Sahu (2009), the liver is the main organ involved in metabolism and detoxification of xenobiotics and can play a major role in the translocation of nanoparticles from the intestinal barrier to the bloodstream. Moreover, the kidneys play a significant role for renal filtration. Our results showed that parameters of renal function (CRE and BUN) return to normal (comparable to the control group) after 21 days from the administration. As a result of this study, after the evaluation of liver and kidney functions

it could be concluded that the rate of D-IONPs metabolism in liver and kidney is dependent to the time interval from administration. According to Farag et al. (2006) and Patel et al. (2008), the tests of liver and kidney functions are significant parameters in determining the security of functional ingredient or final product.

With regards to the histopathological examination, the monocytes, eosinophils, neutrophils, lymphocytes were not observed after 7 days from administration of the nanoparticles. The lack of monocytes demonstrates that the acute inflammatory reaction was not induced in the organs after 7 days. The histopathological examination of liver and kidney sections from injected rats showed normal architecture 21 days after injection. The sections showed that in the liver and kidney tissues no area of necrosis was seen at 1, 7 or 14 days after injection. In injected rats, no significant pathological changes in liver and kidneys were observed after 21 days, in good agreement with the biochemical analysis of blood.

In the early 90s, Weissleder et al. (1990) in their studies showed that superparamagnetic iron oxide particles are not instantly acknowledged by the splenic and hepatic mononuclear phagocytic systems. Later, Kooi et al. (2003) in their studies showed that nanoscale magnetic particles could be assimilated by the entire body due to their non-recognition by the splenic and hepatic mononuclear phagocytic systems. On the other hand, Schulze et al. (1995) in their studies showed that 89% of dextran coating is eliminated in urine, and the rest is excreted in feces. More than that, the iron contained in USPIO is incorporated into the body's iron store and used in hemoglobin manufacture (Weissleder et al. 1989). But then, Cho et al. (2009) showed that the instilled Cy5.5-conjugated TCL-SPION entered into systemic circulation and excreted by urine without accumulation in any other organs except for the kidneys.

With regard to our studies, we could say that the toxicity of the nanoparticles depends on surface chemistry and/or particle size. For all the tested concentrations, the D-IONPs did not present any toxic effect. The renal and liver functions were in the normal range as reported to the control group, suggesting that surface chemistry and particle size are crucial factors in the determination of glomerular filtration. For a correct assessment, further study is needed to establish the influence of different concentrations of D-IONPs in aqueous suspension on *in vivo* tolerability. Considering the fact that the males and females rats have a real different catabolism and that the female rats are more resistant to diseases (Rando and Wahli 2011), the latter could dispose differentially the nanoparticles in the organs. Therefore, additional studies are needed to comprehend the *in vivo* behavior of dextran coated iron oxide nanoparticles. Moreover, additional studies are necessary to understand the influence of D-IONPs in the blood stream. Due to the lack of information on toxicity risks of nanoscale materials to humans and the environment,

*in vivo* tests must be conducted taking into account various parameters such as the colloidal stability, size, concentration and the effective coating of nanoparticles. In addition, despite the fact that other studies are needed, our results proved that D-IONPs can be potential materials to be used as diagnostic probes and delivery vehicles.

**Acknowledgments.** This work was financially supported by the project PN II 131/2014.

## References

- Barick K. C., Singh S., Bahadur D., Lawande M. A., Patkar D. P., Hassan P. A. (2014): Carboxyl decorated Fe<sub>3</sub>O<sub>4</sub> nanoparticles for MRI diagnosis and localized hyperthermia. *J. Colloid. Interface Sci.* **418**, 120–125  
<http://dx.doi.org/10.1016/j.jcis.2013.11.076>
- Bautista M. C., Oscar Bomati M., Morales M. P., Serna C. J., Veintemillas-Verdaguer S. (2005): Surface characterization of dextran-coated iron oxide nanoparticles prepared by laser pyrolysis and coprecipitation. *J. Magn. Mater.* **293**, 20–27  
<http://dx.doi.org/10.1016/j.jmmm.2005.01.038>
- Berry C. C., Curtis A. S. G. (2003): Functionalisation of magnetic nanoparticles for applications in biomedicine. *J. Phys. D.* **36**, R198–206  
<http://dx.doi.org/10.1088/0022-3727/36/13/203>
- Chen H., Ebner A. D., Ritter J. A., Kaminske M. D., Rosengart A. J. (2008): Theoretical analysis of a magnetic separator device for ex-vivo blood detoxification. *Sep. Sci. Technol.* **43**, 996–1020  
<http://dx.doi.org/10.1080/01496390801910609>
- Chen Z., Hong G., Hong G., Wang H., Welsher K., Tabakman M. S., Sherlock S. P., Robinson J. T., Liang Y., Dai H. (2012): Graphite-coated magnetic nanoparticle microarray for few-cells enrichment and detection. *ACS Nano* **6**, 10 94–1101  
<http://dx.doi.org/10.1021/nn2034692>
- Cho W. S., Choi M., Han B. S., Cho M., Oh J., Park K., Kim S. J., Kim S. H., Jeong J. (2007): Inflammatory mediators induced by intratracheal instillation of ultrafine amorphous silica particles. *Toxicol. Lett.* **175**, 24–33  
<http://dx.doi.org/10.1016/j.toxlet.2007.09.008>
- Cho W. S., Cho M., Jeong J., Choi M., Cho H. Y., Han B. S., Kim S. H., Kim H. O., Lim Y. T., Chung B. H. (2009a): Acute toxicity and pharmacokinetics of 13 nm-sized PEG-coated gold nanoparticles. *Toxicol. Appl. Pharmacol.* **236**, 16–24  
<http://dx.doi.org/10.1016/j.taap.2008.12.023>
- Cho W. S., Cho M., Kim S. R., Choi M., Lee J. Y., Han B. S., Park S. N., Yu M. K., Jon S., Jeong J. (2009b): Pulmonary toxicity and kinetic study of Cy5.5-conjugated superparamagnetic iron oxide nanoparticles by optical imaging. *Toxicol. Appl. Pharm.* **239**, 106–115  
<http://dx.doi.org/10.1016/j.taap.2009.05.026>
- Choi H. S., Liu W., Misra P., Tanaka E., Zimmer J. P., Itty Ipe B., Bawendi M. G., Frangioni J. V. (2007): Renal clearance of quantum dots. *Nat. Biotechnol.* **25**, 1165–1170  
<http://dx.doi.org/10.1038/nbt1340>

- Crichton R. (2004): *Inorganic Biochemistry of Iron Metabolism*. John Wiley & Sons Ltd, Ellis Horwood: Chichester, UK
- Easo S. L., Mohanan P. V. (2013): Dextran stabilized iron oxide nanoparticles: Synthesis, characterization and in vitro studies. *Carbohydr. Polym.* **92**, 726–732  
<http://dx.doi.org/10.1016/j.carbpol.2012.09.098>
- Elliott S. R. (1984): *Physics of Amorphous Materials*. Longman Group Ltd., London, New York
- Farag R. S., Mahmoud E. A., Basuny A. M., Ali R. F. M. (2006): Influence of crude olive leaf juice on rat liver and kidney functions. *Int. J. Food. Sci. Tech.* **41**, 790–798  
<http://dx.doi.org/10.1111/j.1365-2621.2006.01093.x>
- Handy R. D., Shaw B. J. (2007): Toxic effects of nanoparticles and nanomaterials: Implications for public health, risk assessment and the public perception of nanotechnology. *Health. Risk. Soc.* **9**, 125–144  
<http://dx.doi.org/10.1080/13698570701306807>
- Hara K., Tsujimoto H., Tsukada Y., Huang C.C., Kawashima Y., Tsutsumi M. (2008): Histological examination of PLGA nanospheres for intratracheal drug administration. *Int. J. Pharm.* **356**, 267–273  
<http://dx.doi.org/10.1016/j.ijpharm.2007.12.041>
- Huang C., Tang Z., Zhou Y., Zhou X., Jin Y., Li D., Yang Y., Zhou S. (2012): Magnetic micelles as a potential platform for dual targeted drug delivery in cancer therapy. *Int. J. Pharm.* **429**, 113–122  
<http://dx.doi.org/10.1016/j.ijpharm.2012.03.001>
- Hudson J. Q., Comstock T. J. (2001): Considerations for optimal iron use for anemia due to chronic kidney disease. *Clin. Ther.* **23**, 1637–1671  
[http://dx.doi.org/10.1016/S0149-2918\(01\)80135-1](http://dx.doi.org/10.1016/S0149-2918(01)80135-1)
- Iconaru S. L., Prodan A. M., Motelica-Heino M., Sizaret S., Predoi D. (2012): Synthesis and characterization of polysaccharide-maghemite composite nanoparticles and their antibacterial properties. *Nanoscale Res. Lett.* **7**, 576–584  
<http://dx.doi.org/10.1186/1556-276X-7-576>
- Jain T. K., Morales M. A., Sahoo S. K., Leslie-Pelecky D. L., Labhasetwar V. (2005): Iron oxide nanoparticles for sustained delivery of anticancer agents. *Mol. Pharm.* **2**, 194–205  
<http://dx.doi.org/10.1021/mp0500014>
- Jun Y. W., Seo J. W., Cheon J. (2008): Nanoscaling laws of magnetic nanoparticles and their applicabilities in biomedical science. *Acc. Chem. Res.* **41**, 179–189  
<http://dx.doi.org/10.1021/ar700121f>
- Kane R. C. (2003): Intravenous iron replacement with sodium ferric gluconate complex in sucrose for iron deficiency anemia in adults. *Curr. Ther. Res. Clin. Exp.* **64**, 263–268  
[http://dx.doi.org/10.1016/S0011-393X\(03\)00038-9](http://dx.doi.org/10.1016/S0011-393X(03)00038-9)
- Kim J. S., Yoon T. J., Yu K. N., Kim B. G., Park S. J., Kim H. W., Lee K. H., Park S. B., Lee J. K., Cho M. H. (2006). Toxicity and tissue distribution of magnetic nanoparticles in mice. *Toxicol. Sci.* **89**, 338–347  
<http://dx.doi.org/10.1093/toxsci/kfj027>
- Kinsella J. M., Ivanisevic A. (2005): Enzymatic clipping of DNA wires coated with magnetic nanoparticles. *J. Am. Chem. Soc.* **127**, 3276–3277  
<http://dx.doi.org/10.1021/ja043865b>
- Kooi M. E., Cappendijk V. C., Cleutjens K. B., Kessels A. G., Kitslaar P. J., Borgers M., Frederik P. M., Daemen M. J., van Engelsehoven J. M. (2003): Accumulation of ultrasmall superparamagnetic particles of iron oxide in human atherosclerotic plaques can be detected by in vivo magnetic resonance imaging. *Circulation* **107**, 2453–2458  
<http://dx.doi.org/10.1161/01.CIR.0000068315.98705.CC>
- Kwon J. T., Hwang S. K., Jin H., Kim D. S., Minai-Tehrani A., Yoon H. J., Choi M., Yoon T. J., Han D. Y., Kang Y. W., Yoon B. I., Lee J. K., Cho M. H. (2008): Body distribution of inhaled fluorescent magnetic nanoparticles in the mice. *J. Occup. Health* **50**, 1–6  
<http://dx.doi.org/10.1539/joh.50.1>
- Laurent S., Mahmoudi M. (2011): Superparamagnetic iron oxide nanoparticles: promises for diagnosis and treatment of cancer. *Int. J. Mol. Epidemiol. Genet.* **2**, 367–390
- Lee H., Lee E., Kim D. K., Jang N. K., Jeong Y. Y., Jon S. (2006): Antibiofouling polymer-coated superparamagnetic iron oxide nanoparticles as potential magnetic resonance contrast agents for in vivo cancer imaging. *J. Am. Chem. Soc.* **128**, 7383–7389  
<http://dx.doi.org/10.1021/ja061529k>
- Pankhurst Q. A., Connolly J., Jones S. K., Dobson J. (2003): Applications of magnetic nanoparticles in biomedicine. *J. Phys. D.* **36** R167  
<http://dx.doi.org/10.1088/0022-3727/36/13/201>
- Patel C., Dadhaniya P., Hingorani L., Soni M. G. (2008): Safety assessment of pomegranate fruit extract: acute and subchronic toxicity studies. *Food. Chem. Toxicol.* **46**, 2728–2735  
<http://dx.doi.org/10.1016/j.fct.2008.04.035>
- Paul K. G., Frigo T. B., Groman J. Y., Groman E. V. (2004): Synthesis of ultrasmall superparamagnetic iron oxides using reduced polysaccharides. *Bioconjug. Chem.* **15**, 394–401  
<http://dx.doi.org/10.1021/bc034194u>
- Petri-Fink A., Hofmann H. (2007): Superparamagnetic iron oxide nanoparticles (SPIONs): from synthesis to in vivo studies – a summary of the synthesis, characterization, in vitro, and in vivo investigations of SPIONs with particular focus on surface and colloidal properties. *IEEE. Trans. Nanobioscience* **6**, 289–297  
<http://dx.doi.org/10.1109/TNB.2007.908987>
- Predoi D. (2007): A study on iron oxide nanoparticles coated with dextrin obtained by coprecipitation. *Dig. J. Nanomater. Bios.* **2**, 169–173
- Predoi D., Valsangiacom C. M. (2007): Thermal studies of magnetic spinel iron oxide in solution. *J. Optoelectron. Adv. M.* **9**, 1797–1799
- Rando G., Wahli W. (2011): Sex differences in nuclear receptor-regulated liver metabolic pathways. *Biochim. Biophys. Acta.* **1812**, 964–973  
<http://dx.doi.org/10.1016/j.bbadis.2010.12.023>
- Rochelle Arvizo R., De M., Rotello M. V. (2007): Proteins and nanoparticles: covalent and noncovalent conjugates. In: *Nanobiotechnology II: More Concepts and Applications*. (Eds. C. A. Mirkin and C. M. Niemeyer), Wiley-VCH, Weinheim, Germany  
<http://dx.doi.org/10.1002/9783527610389.ch4>
- Sahu S. (2009): Hepatotoxic potential of nanomaterials. In: *Nanotoxicity: From In Vivo and In Vitro Models to Health Risks*. John Wiley & Sons, Chichester  
<http://dx.doi.org/10.1002/9780470747803.ch10>

- Schulze E., Ferrucci J. T., Poss K., Lapointe L., Bogdanova A., Weissleder R. (1995): Cellular uptake and trafficking of a prototypical magnetic iron oxide label in vitro. *Invest. Radiol.* **30**, 604–610  
<http://dx.doi.org/10.1097/00004424-199510000-00006>
- Shapiro E. M., Skrtic S., Koretsky A. P. (2005): Sizing it up: cellular MRI using micron-sized iron oxide particles. *Magn. Reson. Med.* **53**, 329–338  
<http://dx.doi.org/10.1002/mrm.20342>
- Su B., Xiang S. L., Su J., Tang H. L., Liao Q. J., Zhou Y. J., Qi S. (2012): Diallyl disulfide increases histone acetylation and P21WAF1 expression in human gastric cancer cells in vivo and in vitro. *Biochem. Pharmacol.* **1**, 1–10  
<http://dx.doi.org/10.4172/2167-0501.1000106>
- Stamopoulos D., Benaki D., Bouziotis P., Ziogiannis P. N. (2007): In vitro utilization of ferromagnetic nanoparticles in hemodialysis therapy. *Nanotechnology* **18**, 495102  
<http://dx.doi.org/10.1088/0957-4484/18/49/495102>
- Stamopoulos D., Manios E., Gogola V., Benaki D., Bouziotis P., Niarchos D., Pissas M. (2008): Bare and protein-conjugated Fe(3)O(4) ferromagnetic nanoparticles for utilization in magnetically assisted hemodialysis: biocompatibility with human blood cells. *Nanotechnology* **19**, 505101  
<http://dx.doi.org/10.1088/0957-4484/19/50/505101>
- Sun S., Zeng H. (2002): Size-controlled synthesis of magnetite nanoparticles. *J. Am. Chem. Soc.* **124**, 804–805  
<http://dx.doi.org/10.1021/ja026501x>
- Tartaj P., Morales M. P., Veintemillas-Verdaguer S., Gonzalez-Carreno T., Serna C. J. (2003): The preparation of magnetic nanoparticles for applications in biomedicine. *J. Phys. D.* **36**, R182–197  
<http://dx.doi.org/10.1088/0022-3727/36/13/202>
- Thorek D. L. J., Tsourkas A. (2008): Size, charge and concentration dependent uptake of iron oxide particles by non-phagocytic cells. *Biomaterials* **29**, 3583–3590  
<http://dx.doi.org/10.1016/j.biomaterials.2008.05.015>
- Weissleder R., Hahn P. F., Stark D. D., Elizondo G., Saini S., Todd L. E., Wittenberg J., Ferrucci J. T. (1988): Superparamagnetic iron oxide: enhanced detection of focal splenic tumors with MR imaging. *Radiology* **169**, 399–403  
<http://dx.doi.org/10.1148/radiology.169.2.3174987>
- Weissleder R., Stark D. D., Engelstad B. L., Bacon B. R., Compton C. C., White D. L., Jacobs P., Lewis J. (1989): Superparamagnetic iron oxide: pharmacokinetics and toxicity. *AJR Am. J. Roentgenol.* **152**, 167–173  
<http://dx.doi.org/10.2214/ajr.152.1.167>
- Weissleder R., Elizondo G., Wittenberg J., Rabito C. A., Bengel H. H., Josephson L. (1990): Ultrasmall superparamagnetic iron oxide: characterization of a new class of contrast agents for MR imaging. *Radiology* **175**, 489–493  
<http://dx.doi.org/10.1148/radiology.175.2.2326474>
- Yallapu M. M., Othman S. F., Curtis E. T., Gupta B. K., Jaggi M., Chauhan S. C. (2011): Multi-functional magnetic nanoparticles for magnetic resonance imaging and cancer therapy. *Biomaterials* **32**, 1890–1905  
<http://dx.doi.org/10.1016/j.biomaterials.2010.11.028>
- Yang R. S., Chang L. W., Wu J. P., Tsai M. H., Wang H. J., Kuo Y. C., Yeh T. K., Yang C. S., Lin P. (2007): Persistent tissue kinetics and redistribution of nanoparticles, quantum dot **705**, in mice: ICP-MS quantitative assessment. *Environ. Health Perspect.* **115**, 1339–1343  
<http://dx.doi.org/10.1289/ehp.10290>
- Yigit M. V., Mazumdar D., Lu Y. (2008): MRI detection of thrombin with aptamer functionalized superparamagnetic iron oxide nanoparticles. *Bioconjugate Chem.* **19**, 412–417  
<http://dx.doi.org/10.1021/bc7003928>
- Zhang X., Niu H., Yan J., Cai Y. (2011): Immobilizing silver nanoparticles onto the surface of magnetic silica composite to prepare magnetic disinfectant with enhanced stability and antibacterial activity. *Colloids Surf. A* **375**, 186–192  
<http://dx.doi.org/10.1016/j.colsurfa.2010.12.009>

Received: August 26, 2015

Final version accepted: January 16, 2016

First published online: April 5, 2016